X-ray Absorption near Edge Structure and Extended X-ray Absorption Fine Structure Analysis of Fe(II) Aqueous and Acetone Solutions

ARTICLE *in* THE JOURNAL OF PHYSICAL CHEMISTRY A · NOVEMBER 2011

Impact Factor: 2.69 · DOI: 10.1021/jp207587u · Source: PubMed

4 AUTHORS, INCLUDING:

Wojciech Olszewski
Cells Alba
30 PUBLICATIONS **76** CITATIONS

SEE PROFILE

THE JOURNAL OF PHYSICAL CHEMISTRY A

ARTICLE

pubs.acs.org/JPCA

X-ray Absorption near Edge Structure and Extended X-ray Absorption Fine Structure Analysis of Fe(II) Aqueous and Acetone Solutions

Wojciech Olszewski,*[,†] Krzysztof Szymański,[†] Piotr Zaleski,[†] and Dariusz A. Zając[‡,§]

[†]Faculty of Physics, University of Bialystok, Lipowa 41, 15-424 Białystok, Poland

[‡]Deutsches Elektronen-Synchrotron-Hasylab, Notkestrasse 85, 22607 Hamburg, Germany

[§]H. Niewodniczański Institute of Nuclear Physics of PAN, Radzikowskiego 152, 31-342 Kraków, Poland

ABSTRACT: X-ray absorption spectroscopy measurements were used to determine the structure of the first coordination shell of Fe(II) ions in aqueous and acetone based solutions. Extended X-ray absorption fine structure analysis coupled with ab initio X-ray absorption near edge structure calculations confirms the octahedral coordination of the iron ion in water based solution. Data collected for acetone rich solutions can be reproduced assuming coexistence of the octahedral $Fe(H_2O)_6^{2+}$ and tetrahedral $[FeCl_4]^{2-}$ complexes. Distortion of the tetrahedral coordination of ion was detected in some of the acetone based solutions.

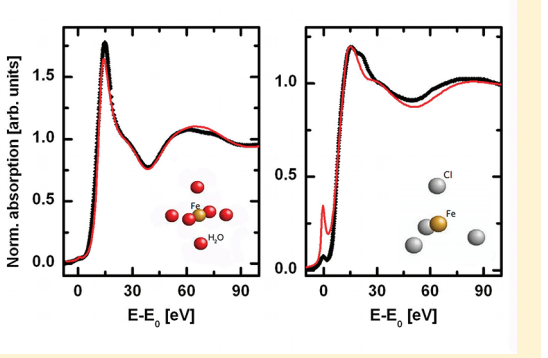

1. INTRODUCTION

Fe layers and nanocrystals attract considerable interest for fundamental and applied research due to new technologies for advanced materials and application.[1,2] One of the easiest ways to obtain the metallic layers is electrodeposition from commonly used aqueous solutions of chloride[3] or sulfamate.[4] Recently, electroplating of shiny layers from a new type of electrolyte consisting mainly of acetone was developed.[5,6] Under the same dc current conditions we can obtain shiny layers of Fe, Co, Ni, Cu, and Zn well connected to the substrate. The electrodeposition process from acetone based solution stops at a thickness of a few hundred nanometers.[7] Additionally, Mössbauer measurements of the obtained iron layers show that the magnetic moments have small preferential orientation, perpendicular to the sample plane, a result rather unexpected in the case of layers as thick as few hundred nanometers. Also, when the concentration of water in acetone based electrolyte is too small, the electroplating of metal layer is not possible.

The differences between water and acetone based solutions motivated us to study the local structure of Fe(II) complexes in those electrolytes. The structural properties of the first hydration shell of 3d ions, including Fe(II),[8] are known reasonably well.[9,10] In contrast, the nearest environment of Fe(II) in acetone solutions has not been reported so far and that knowledge may contribute to a better understanding of the kinetics of electrodeposition processes. The X-ray absorption spectroscopy (XAS) technique is an excellent method for the investigation of the local structure of ions.

2. X-RAY ABSORPTION SPECTROSCOPY

XAS is a powerful technique that provides element sensitive information on the nearest environment and electronic structure of the condensed matter. The principles of XAS are based on the interactions of X-rays with matter. Due to photoelectrical effect, in which an X-ray is absorbed by a core-level with binding energy, a photoelectron with wavenumber k is created and propagates away from the atom to the continuum. This photoelectron wave interferes with wave scattered by the electrons of neighboring atoms, altering the absorption coefficient (μ). An XAS measurement is simply a measure of the energy dependence of μ at and above the binding energy of a known core level of a known atomic species. Because every atom has core-level electrons with well-defined binding energies, by tuning the X-ray energy to an appropriate absorption edge, an element can be selected. XAS spectroscopy covers both the X-ray absorption near edge structure (XANES) and the extended X-ray absorption fine structure (EXAFS), having the same physical origin.

The XANES is the part of the absorption spectrum near an absorption edge (approximately −50 to +100 eV relative to the edge energy). The binding geometry and the oxidation state of the atom directly affect the XANES part of the spectrum. The main "steplike" feature of the absorption edge is due to the excitation of the photoelectron into the continuum. The absorption edge for some elements includes some extra features. These may be isolated peak(s), shoulder(s), or a strong peak at the top

Received: August 8, 2011
Revised: October 12, 2011
Published: October 13, 2011

Table 1. Composition of Examined Solutions

	concentration (mol/dm^3)			
solution	$FeCl_2$	HCl	H_2O	C_3H_6O
1	0.03	0.12	55.39	0
2	0.03	0.10	2.88	12.90
3	0.03	0	0.12	13.60

of the step, called a white line. These features are caused by differences in the density of unoccupied electron orbitals that can be occupied by the excited photoelectron, and are a function of the cluster geometry and absorber redox state. Increase of the oxidation state results in a positive shift of the energy edge providing a direct fingerprint of redox state.

The EXAFS is the oscillatory part of the absorption coefficient above the absorption edge. The EXAFS spectrum contains information on the number of different coordinating species and their distances to the absorber atom, angles between chemical bonds and thermal disorder. The EXAFS oscillations result from the interference between scattered and not scattered electronic waves which are shifted in phase by scattering mechanisms.

3. MATERIALS AND METHODS

3.1. Sample Preparation. The first studied sample (**1**), consists of $FeCl_2 \cdot 4H_2O$ dissolved in water with a small amount of HCl, and it serves as reference. Acetone based electrolyte for metallic layer deposition[6] consists of small amount of $FeCl_2$, HCl, and water dissolved in acetone and was the second studied sample (**2**). The third sample served again as kind of reference and was prepared by dissolving of small amount of $FeCl_2 \cdot 4H_2O$ and water in acetone (**3**). The iron concentration was the same in all three samples and the compositions are shown in Table 1. All samples were prepared carefully to avoid oxidation of Fe(II) to Fe(III).

After preparation, the electrolytes were transferred to the nonmetallic cells prepared for XAS measurements of liquid samples. The body of this cell consists of a hollow Teflon cylinder (o.d. 49 mm, i.d. 16 mm) with a thickness of 10 mm. The inner ring of this cell is the sample chamber. Two Kapton disks are the cell windows.

3.2. X-ray Absorption Measurements. XAS measurements at the Fe K-edge were performed in transmission mode at the E4 and A1 stations of HASYLAB (DESY, Germany). The storage ring was operating at a position beam energy of 4.5 GeV. The radiation was monochromatized by a double-crystal, fixed end, Si(111) monochromator. The intensities of incident and transmitted beams were monitored by ionization chambers filled with N_2 gas. The XAS spectra were recorded at room temperature. Energy calibration of all spectra was achieved by simultaneous measurements of absorption near Fe K-edge (7112 eV) of a reference 5 μm Fe foil.

3.3. Data Analysis. Simulations of Fe K-edge XANES have been performed by the FDMNES code.[11] Instead of commonly used locally spherically symmetric muffin-tin (MT) approximation, the finite difference method (FDM)[12] with the real energy-dependent exchange Hedin−Lundqvist (H-L) potential[13] was adopted for calculations of the nonspherical electron distribution.

During the calculation the FDMNES spectra were convolved with a 1.25 eV Lorentzian distribution to simulate the core-hole

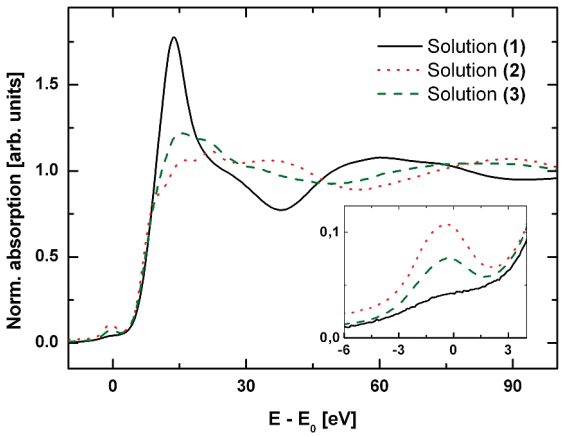

Figure 1. Normalized *K*-edge absorption spectra of Fe(II) in water−acetone solutions. The inset shows enlarged pre-edge region.

width[14] and a 1 eV Gaussian distribution for the experimental broadening. Those values were set a priori and were not changed during the data analysis.

The extended parts of the data were analyzed by means of the GNXAS code.[15,16] Phase shifts were calculated using MT approximation with H-L potential. The values of the MT radii were 0.2, 0.9, 1.1, and 1.2 Å for hydrogen, oxygen, chlorine, and iron, respectively. The MT radius chosen for the hydrogen atoms does not overestimate the signal from the scattering of hydrogen atoms, which is expected to be weak. This value has been successfully used in previous quantitative EXAFS data analysis of 3d metal transition ions in solutions.[17,18]

4. RESULTS AND DISCUSSION

4.1. Qualitative Interpretation. The shape of normalized Fe K-edge XANES spectra depends strongly on the water concentration (Figure 1). The shape of the spectra of solution **1** confirms that in aqueous solution Fe(II) ions exist as octahedral $Fe(H_2O)_6^{2+}$ complexes.[9,19] The weak pre-edge peak in XANES spectrum of solution **1** is due to quadrupolar transition in octahedral ion coordination. In the case of noncentrosymmetric tetrahedral coordination, by a mixing of 4p and 3d orbitals, the dipolar 1s−3d transition is allowed, causing the increase of the pre-edge peak intensity.[20] We observe an apparent pre-edge peak (inset of Figure 1) in solutions **2** and **3** with large acetone concentrations. Also, the intensity of the white line (corresponding to the 1s−4p dipolar transition) is reduced for solutions poor in water, which is consistent with results of observations of tetrahedral structures.[21]

It is interesting to note that the shapes of the spectra do not change systematically with water concentration. In solution **3** the prepeak intensity, the white line amplitude, and the intensity in extended region is roughly between those observed in **1** and **2**.

4.2. Quantitative EXAFS Anlaysis. The EXAFS data of Fe(II) in different solutions were analyzed over the range $k = 3-14$ Å^{-1}. Data for further analysis was obtained from the experimental signal by approximating and subtracting a smooth tree-segmented spline function. In the upper panels of Figure 2 the comparison between experimental signals and theoretical EXAFS curves is shown. The first curves from the top of each panel are the two body Fe−O, Fe−Cl, or Fe−H first shell contributions and, in the case of the first panel, the multiple scattering

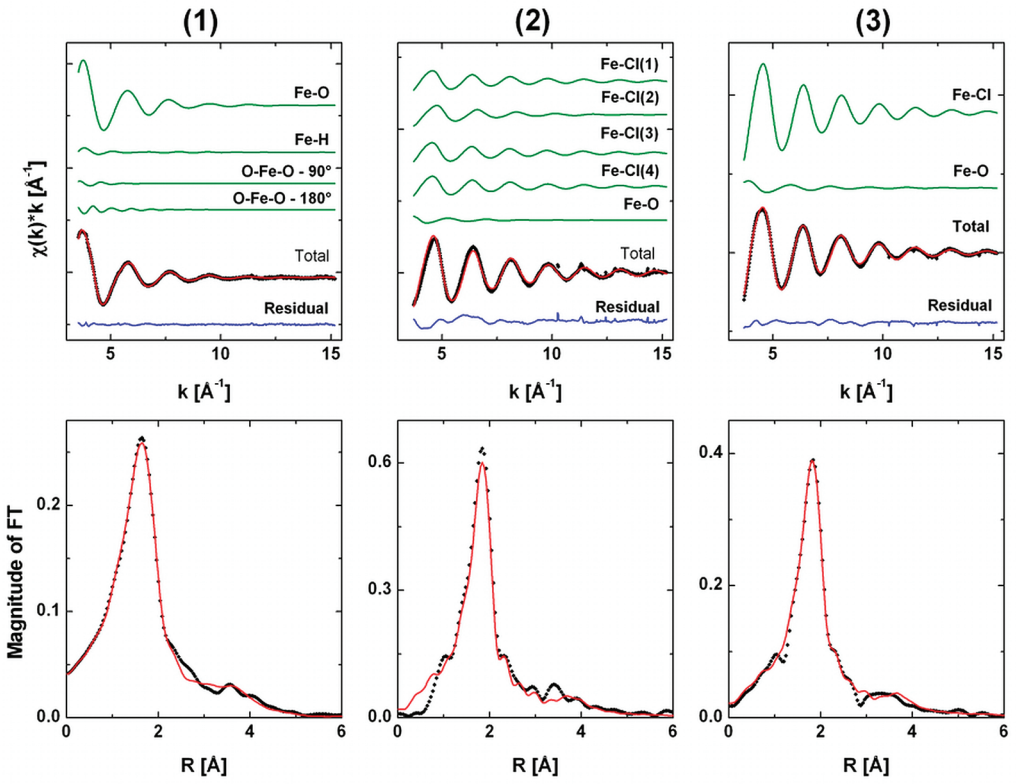

Figure 2. Top panels: best fit of EXAFS $\chi(k)\cdot k$ spectra at the Fe *K*-edge of Fe(II) ion in solutions **1**−**3**, respectively. Bottom panels: FT of the experimental data (dotted line) and total theoretical signals (full line).

Table 2. Structural Parameters for Fe(II) in Water 1 and Acetone Based Solutions 2 and 3 Obtained from the EXAFS Data Analysis[a]

	proposed model			structural parameters		
	complex symmetry	percentage composition	shell	*N*	*R* (Å)	σ^2
solution **1**	octahedron	100	Fe−O	6	2.12(1)	0.0073(3)
			Fe−H	12	2.78(5)	0.0116(5)
solution **2**	distorted tetrahedron	90	Fe−Cl(1)	1	2.23(3)	0.0049(6)
			Fe−Cl(2)	1	2.11(6)	0.0048(9)
			Fe−Cl(3)	1	2.21(3)	0.0049(6)
			Fe−Cl(4)	1	2.21(3)	0.0049(6)
	octahedron	10	Fe−O	6	2.15(4)	0.0066(4)
solution **3**	tetrahedron	80	Fe−Cl	4	2.20(4)	0.0045(5)
	octahedron	20	Fe−O	6	2.14(2)	0.0061(3)

[a] The parameters are the coordination number (*N*), the distance to the scattering shell (*R*) and the EXAFS Debye−Waller factor (σ^2).

signals associated with the linear and the orthogonal O−Fe−O configurations. Comparison of the calculated curves with experimental points as well as the residuals are shown at the bottom of the upper panels. All signals are multiplied by *k* for better visualization. Values of the obtained structural parameters for each solution are listed in Table 2.

The EXAFS spectrum of solution **1** can be reproduced well by an octahedral environment of the Fe(II) ion as reported by Benfatto et al.[9] As expected, the dominant contribution to the total EXAFS spectrum is given by the Fe−O first shell signal. The contribution of Fe−H and the two-body scattering cannot be neglected. Obtained parameters (Table 2) are in agreement with results reported previously: $d_{Fe(II)-O}$ = 2.10(6) Å;[8] $d_{Fe(II)-O}$ = 2.12(1) Å, $d_{Fe(II)-H}$ = 2.85(5) Å.[22]

In the analysis of solutions **2** and **3**, the coexistence of two different surroundings of iron ion have to be assumed. A total of 80−90% of the Fe(II) ions form tetrahedral $[FeCl_4]^{2-}$ species and 10−20% octahedral $Fe(H_2O)_6^{2+}$. The Fe−O distances, within the experimental accuracy, are the same in all solutions. In solution **2** the tetrahedron, formed by four chloride ions is slightly deformed. As can be seen in Table 2, one of the bonds is shorter than the other three (with equal lengths). Thus decrease

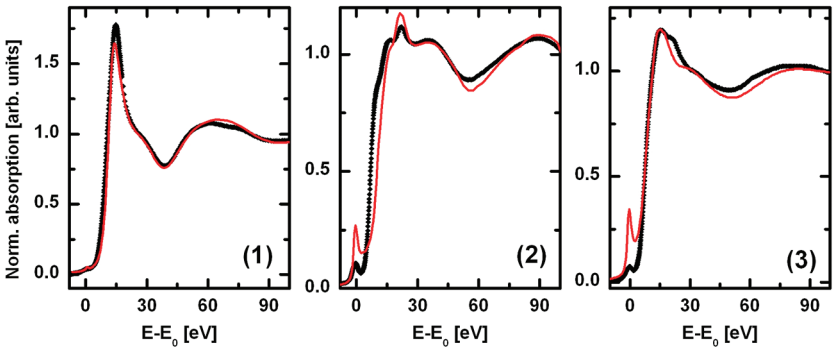

Figure 3. Comparison of the theoretical XANES calculations with experimental data obtained for investigated solutions **1**−**3**, respectively.

of the water concentration results in a change of the tetrahedral surrounding of the iron ion to more symmetrical without observable distortions.

The two-body Cl−Fe−Cl signals are too weak to bring significant changes to the total signal. This is expected because Fe−Cl bonds in tetrahedral arrangements does not form a 180° angle. Also the small amount of Fe(II) octahedral species (10−20%) results in very weak signal associated with Fe−H and O−Fe−O scattering. For this reason those signals were not included in final calculations.

The quality of the fit can also be seen at the non-phase-shift-corrected Fourier transform (FT) of the experimental and theoretical signals (lower panels of Figure 2). The FT spectra show one main peak that is due to first shell distance.

Overall, the calculated EXAFS spectra match the experimental data reasonably well in all cases, showing the consistency of proposed local structure. The obtained values of structural parameters are in good agreement with those obtained for Fe(II) in brines: $d_{Fe(II)-Cl}$ = 2.31(5) Å[21] and the average value: $d_{Fe(II)-Cl}$ = 2.29 Å found in the crystallographic study of $[N(CH_3)_4]_2[FeCl_4]$.[23]

4.3. Ab Initio XANES Calculations. Local structures and the parameters extracted in EXAFS analysis (Table 2) were used for ab initio calculations of XANES spectra shown in Figure 3.

The XANES spectrum calculation for solution **1** was based on $Fe(H_2O)_6^{2+}$. Both the pre-edge and postedge regions of the spectrum are well reproduced, except for two small discrepancies (Figure 3). First the intensity of the white line is underestimated in the theoretical spectrum. As was shown by D'Angelo et al.,[24] this is due to neglecting the disordered second hydration shell. The second disagreement between theoretical and experimental spectra occurs at 60 eV above the absorption edge. The reason for this behavior is the presence of the 1s−3s multielectron excitation edge,[22] which is not included in the FDMNES code.

According to the EXAFS analysis in solution **2**, 90% of iron cations form a slightly distorted tetrahedral configuration with chloride ions and the remaining 10% octahedral $Fe(H_2O)_6^{2+}$ species. As can be seen in the second graph in Figure 3, the agreement between theoretical calculations and experimental data is pretty good. Above 15 eV, the position and relative intensities of the oscillations match the experimental data. Again the amplitude of the oscillations is larger than the experimental one, possibly due to the absence of thermal disorder in presented simulations. The pre-edge region is well reproduced. Some small disagreement between theoretical calculations and experimental spectrum exists. The shoulder detected experimentally at energy $E - E_0$ = 11 eV is not reproduced in the calculations. One possible explanation of this feature can be the presence of $[FeCl_3]^-$ complex. As it was shown by Testamale et al.,[21] the trigonal $FeCl_3$ structure gives rise to a shoulder of the white line and the rest of the spectrum remains similar to that for the tetrahedral $FeCl_4$ cluster. Unfortunately, the intensity of the shoulder is not high enough to reproduce the presented data well. That is why the origin of this feature is still under investigation.

In the case of solution **3**, a combination of two different local surroundings of the iron ions was used to reproduce the obtained experimental result. As was shown in the previous section, we assumed that 80% of iron ions form tetrahedral $[FeCl_4]^{2-}$ species and 20% of the ions tend to form octahedral complexes with water molecules. As can be seen, the agreement between the theoretical signal and the experimental data is good (last panel in Figure 3) except for some small discrepancies. The first one, located around 50 eV above the absorption edge, is most probably a result of thermal fluctuations. Another one is located in the white line region. Lack of small bump on the high energy side of the white line could have its origin in the influence of the second hydration shell in this region of the spectrum.

Good agreement between experimental results and local structure proposed in Table 2 and Figures 2 and 3 for solution **3** convince us that, in water deficient or acetone rich solution, tetrahedral $[FeCl_4]^{2-}$ complexes are formed. However, quantitative results presented in Table 2 for solution **3** show that 80% of Fe(II) ions form $[FeCl_4]^{2-}$ complexes and the amount of complexed chloride anions exceed the total amount of chorine anions present in the solution by 60%. A possible explanation of the discrepancy is the following. In the case of low-dielectric nonaqueous solvents, it is possible that the iron chloride may exist in oligomeric forms, for example, iron(III) chloride dimers or polymers in benzene, nitrobenzene, acetone, and others.[25] The presence of Fe_2Cl_6 dimers or Fe_3Cl_8 trimers will not change the results of the XAS analysis (the local surrounding of iron ion is still tetrahedral $FeCl_4$) but will lower the ratio of the Fe to Cl ions. Therefore, in the case of solution **3**, it is probable that 80% of iron ions exist in solution as $FeCl_4$ oligomers and 20% as octahedral complexes with water molecules.

5. SUMMARY

A measurements of XAS spectra of Fe(II) water and acetone based solutions have been performed. The extended and near edge part of the XAS spectra were compared with results of simulations based on the postulated local structure of Fe(II) ions. The proposed models of the first coordination-shell of iron cation explains the experimental signals with reasonably good

precision. The earlier reported octahedral geometry of the first hydration shell in the case of Fe(II) in aqueous solution was confirmed. In acetone rich solutions part of Fe(II) forms $[FeCl_4]^{2-}$ complexes with tetrahedral Cl^- arrangement.

AUTHOR INFORMATION

Corresponding Author
*E-mail: wojtek@alpha.uwb.edu.pl. Tel: +48 85/745 72 42. Fax: +48 85/745 72 23.

ACKNOWLEDGMENT

We express our gratitude to Dr. Hab. E. Jartych from the Technical University of Lublin for valuable discussions on electroplating from water based solution and to Prof. Dr. Hab. K. Jabłońska for suggestions and discussions at the initial stage of the project. Portions of this research were carried out at the light source DORIS III at DESY, a member of the Helmholtz Association (HGF). We would like to thank E. Welter for assistance in using beamline A1. This work was supported by the I-20080184 EC project and the funds allocated for scientific research for the years 2008-2011 as a research project NN202172335.

REFERENCES

(1) Gomez, E.; Pellicer, E.; Duch, M.; Esteve, J.; Valles, E. *Electrochim. Acta* **2006**, *51*, 3214–3222.
(2) Datta, M. *Electrochim. Acta* **2003**, *48*, 2975–2985.
(3) Jartych, E.; Chocyk, D.; Budzyński, M.; Jałochowski, M. *Appl. Surf. Sci.* **2001**, *180*, 246–254.
(4) Se, Moo Hong; Kim, Dong Jin; Kim, Joung Soo *Thin Solid Films* **2005**, *489*, 122–129.
(5) Olszewski, W.; Szymański, K.; Biernacka, M.; Sobiecki, R. *Mater. Sci.-Poland* **2008**, *26*, 743–750.
(6) Szymański, K.; Olszewski, W. Polish Patent No. 207757, 2007.
(7) Olszewski, W.; Szymański, K.; Satuła, D.; Biernacka, M.; Talik, E. K. *Acta Phys. Pol., A* **2008**, *114*, 1631–1640.
(8) Garcia, J.; Bianconi, A.; Benfatto, M.; Natoli, C. R. *J. Phys. Colloq.* **1986**, *47*, C8−49–C8−54.
(9) Benfatto, M.; Solera, J. A.; Chaboy, J.; Proietti, M. G.; Garcia, J. *Phys. Rev. B* **1997**, *56*, 2447–2452.
(10) D'Angelo, P.; Benfatto, M.; Della Longa, S.; Pavel, N. V. *Phys. Rev. B* **2002**, *66*, 064209.
(11) Joly, Y. *Phys. Rev. B* **2001**, *63*, 125120.
(12) Joly, Y. *Phys. Rev. B* **1996**, *53*, 13029–13037.
(13) Hedin, L.; Lundqvist, B. I. *J. Phys. C: Solid State Phys.* **1971**, *4*, 2064–2083.
(14) Krause, M. O.; Oliver, J. H. *J. Phys. Chem. Ref. Data* **1979**, *8*, 329–338.
(15) Filipponi, A.; Di Cicco, A.; Natoli, C. R. *Phys. Rev. B* **1995**, *52*, 15122–15134.
(16) Filipponi, A.; Di Cicco, A. *Phys. Rev. B* **1995**, *52*, 15135–15149.
(17) D'Angelo, P.; Barone, V.; Chillemi, G.; Sanna, N.; Meyer-Klaucke, W.; Pavel, N. V. *J. Am. Chem. Soc.* **2002**, *124*, 1958–1967.
(18) Benfatto, M.; D'Angelo, P.; Della Longa, S.; Pavel, N. V. *Phys. Rev. B* **2002**, *65*, 174205.
(19) Baes Jr., C. F.; Mesmer, R. E. *The Hydrolysis of Cations*; Wiley: New York, 1976.
(20) Galoisy, L.; Calas, G.; Arrio, M. A. *Chem. Geol.* **2001**, *174*, 307–319.
(21) Testamale, D.; Brugger, J.; Liu, W.; Etschmann, B.; Hazemann, J.-L. *Chem. Geol.* **2009**, *264*, 295–310.
(22) D'Angelo, P.; Benfatto, M. *J. Phys. Chem. A* **2004**, *108*, 4505–4514.
(23) Lauher, J. W.; Ibers, J. A. *Inorg. Chem.* **1975**, *14*, 348–352.
(24) D'Angelo, P.; Roscioni, O. M.; Chillemi, G.; Della Longa, S.; Benfatto, M. *J. Am. Chem. Soc.* **2006**, *128*, 1853–1858.
(25) Vertes, A.; Nagy-Czakó, I.; Burger, K. *J. Phys. Chem.* **1978**, *82*, 1469–1473.